Materials Science and Engineering C 61 (2016) 351–354

Contents lists available at ScienceDirect

Materials Science and Engineering C

journal homepage: www.elsevier.com/locate/msec

Short communication

# Real-time measurement of protein adsorption on electrophoretically deposited hydroxyapatite coatings and magnetron sputtered metallic films using the surface acoustic wave technique

M. Meininger, T. Schmitz, T. Wagner, A. Ewald, U. Gbureck, J. Groll, C. Moseke *

*Department for Functional Materials in Medicine and Dentistry, School of Dentistry, University of Würzburg, Pleicherwall 2, 97070 Würzburg, Germany*

ARTICLE INFO

*Article history:*
Received 30 July 2015
Received in revised form 9 December 2015
Accepted 28 December 2015
Available online 30 December 2015

*Keywords:*
Physical vapor deposition
Hydroxyapatite
Surface functionalization
Biosensor

ABSTRACT

Surface acoustic wave (SAW) biosensors are highly sensitive for mass binding and are therefore used to detect protein–protein and protein–antibody interactions. Whilst the standard surface of the chips is a thin gold film, measurements on implant- or bone-like surfaces could significantly enhance the range of possible applications for this technique. The aim of this study was to establish methods to coat biosensor chips with Ti, TiN, and silver-doped TiN using physical vapor deposition as well as with hydroxyapatite by electrophoresis. To demonstrate that protein adsorption can be detected on these surfaces, binding experiments with fibronectin and fibronectin-specific antibodies have been performed with the coatings, which successfully proved the applicability of PVD and EPD for SAW biosensor functionalization.



## 1. Introduction

Surface acoustic wave (SAW) technology – as it has been adapted to biochemical applications – is based on the propagation of *Love* waves on the surface of a piezoelectric crystal [1]. Due to the high SAW frequencies the influence of an adsorbed layer on the acoustic energy of the propagating wave is mostly confined to a very narrow interface between the chip surface and the liquid in the flow cell [2], which results in a higher mass sensitivity as compared to quartz crystal microgravimetry with dissipation monitoring [3]. The method records both phase and amplitude signals, which enables the separation of mass and viscosity effects and minimizes the influence of concentration or viscosity changes in the measurement solutions [4,5]. In comparison to optical biosensor techniques, the SAW method does not require particular optical properties of the measured solution, hence also turbid liquids can be applied [3]. SAW techniques in biosensor applications typically use gold surfaces; these are highly inert and provide the possibility to couple self-assembled monolayers (SAM) of thiols [6,7]. Nevertheless, from a biomaterial science point of view it is also interesting to examine other metallic and ceramic coatings, which may serve as model systems for functional material surfaces or the mineral phase of bone, respectively. Although there are various methods to fabricate such coatings, we will focus below on physical vapor deposition (PVD) and electrophoretic deposition (EPD) techniques.

EPD provides the possibility to thoroughly characterize the coating material prior to deposition and to maintain the chemical properties such as stoichiometry and phase composition during the process. The coating material can be prepared with well-defined particle sizes and hence be deposited with controllable film density. Furthermore, electrophoresis of ceramic materials is usually carried out in non-aqueous media, which significantly reduces the electrical current between the electrodes and eliminates the problem of gas bubble formation.

Besides bone-like calcium phosphate coatings, also metallic implant surfaces are interesting subjects for protein adsorption experiments. Particularly titanium is widely used as implant material because of its excellent biocompatibility and its advantageous mechanical properties [8] and can be easily deposited on a variety of substrates by PVD techniques. PVD methods have also been utilized to fabricate Ti based coatings with antibacterial surface properties, e.g. titanium nitride (TiN) and silver-doped Ti and TiN coatings [9–11]. The aim of this study was to adapt these deposition methods to SAW biosensor chips under consideration of their specific material characteristics. In addition, the feasibility of the SAW technique for protein adsorption measurements on such surface modifications should be proven by model experiments with fibronectin.

## 2. Materials and methods

### 2.1. Electrophoretic deposition

The coating material for the electrophoretic deposition process was hydroxyapatite and was fabricated by the following reaction: 20 wt.%

* Corresponding author.
*E-mail address:* claus.moseke@fmz.uni-wuerzburg.de (C. Moseke).

http://dx.doi.org/10.1016/j.msec.2015.12.075
0928-4931/

phosphoric acid was slowly added to a calcium hydroxide suspension (7.4 g suspended in 200 ml ultrapure water) at 80 °C until a pH value of 8.0 was reached. The obtained suspension was centrifuged, the supernatant decanted, and the precipitated solid washed three times with ethanol and subsequent centrifugation. The final product was suspended in ethanol, filtrated and dried [12]. XRD analysis was performed with a Siemens D5005 diffractometer (Bruker, Karlsruhe, Germany) using Cu-$K_\alpha$ radiation (40 kV acceleration voltage, 40 mA tube current). To obtain additional information about phase composition and purity from thermodynamic decomposition, a powder portion was sintered for 1 h at 1000 °C. For the preparation of the coating electrolyte the as-precipitated HA was ground; then 0.395 g of the powder was suspended with 100 ml ethanol in an ultrasonic bath for 10 min (twice) and subsequently filtered through a suction filter with a pore size of 8–12 μm; the resulting filtrate was then used for the EPD procedure; additional sonication for 10 min was applied immediately before every coating experiment.

Commercially available gold-coated SAW biosensor chips (SAW Instruments GmbH, Bonn, Germany) were used as substrates. Prior to coating the chips were thoroughly pre-cleaned in phosphoric acid, Extran®, SDS, isopropanol, water, and ethanol. Subsequently the chips were treated with a UV/ozone lamp (HNG-Germany) for surface activation. The negative voltage (−100 V/cm) was applied to the uppermost of the five sensor channel areas for 30 s, resulting in HA deposition on the other four channels (see Suppl. Fig. S1). The as-deposited coatings were then densified by immersion in simulated body fluid [13], and afterwards rinsed and dried. The coating topography was analyzed with scanning electron microscopy (SEM CB340, Zeiss, Oberkochen, Germany); the elemental composition was determined by energy-dispersive X-ray spectroscopy (EDS) (XMax$^N$, Oxford-Instruments, Wiesbaden, Germany).

### 2.2. Physical vapor deposition

Deposition of Ti, TiAgN and TiN coatings on the gold surfaces of the SAW biosensor chips was carried out by magnetron sputtering (Pfeiffer Vacuum, Asslar, Germany). Ti and TiN coatings were obtained with a pure Ti target; TiAgN coatings were deposited by sputtering modular TiAg targets [11]. Applied powers were 400 W for TiN and TiAgN and 500 W for Ti. The deposition of the pure Ti layer onto the SAW biosensor was achieved by sputtering for 2 h at an argon pressure of $6.6 \cdot 10^{-3}$ mbar; TiN and TiAgN were deposited with intermediate layers of Ti, respectively TiAg, followed by reactive sputtering in $Ar/N_2$ (flow rate ratio ~14:1, pressure $6.7 \cdot 10^{-3}$ mbar) atmosphere for 60 min. All coatings were deposited without bias voltage, but with a substrate temperature of about 180 °C. X-ray diffraction patterns of the resulting coatings were recorded in grazing angle geometry at a fixed Θ angle of 1°, in order to improve the peak intensities of the coating in relation to the peaks of the gold substrate. Surface topography was examined by atomic force microscopy (Nanosurf AG, Liestal, Switzerland). In tapping mode an area of about 5 μm × 5 μm was measured with a Tap190Al-G cantilever (Budget Sensors, Sofia, Bulgaria) and a resolution of 512 points per line at 700 ms per line.

### 2.3. Protein and antibody adsorption

Adsorption measurements were performed with a Sam5 Blue biosensor (SAW Instruments GmbH, Bonn, Germany) using phosphate buffered saline (PBS) as running buffer. The test solutions were prepared by dissolution in PBS: fibronectin: 50 μg/ml and 300 μg/ml; bovine serum albumin (BSA, Sigma, Taufkirchen, Germany): 1 mg/ml; antibodies MAB (MAB1936, clone 616 (CHEMICON International, Hofheim, Germany)), P1H11 sc-18825 and H300 sc-9068 (both from Santa Cruz Biotechnology, Heidelberg, Germany): 1 μg/ml each. At the beginning of each injection sequence, the flow rate of the medium was set to 40 μl/min. After an equilibration time of 10 min the fibronectin solution was injected followed by a pause of 10 min. Then BSA was injected to occupy free adsorption sites, hence avoiding unspecific binding of antibodies. Afterwards the antibody solutions were injected consecutively with pauses of 3 min. To eliminate effects of residual antibodies on subsequent adsorption, the measurements were repeated varying the injection sequence of the antibodies.

## 3. Results and discussion

The HA powder obtained from the acid–base reaction was characterized by XRD prior to electrophoretic deposition. The as-precipitated powder showed all peaks characteristic for HA of moderate crystallinity (Fig. 1a). In order to increase crystallinity and crystallite size and identify the phase purity, the powders were sintered for 1 h at 1000 °C. In the diffraction pattern of the heat-treated powder, the absence of additional phases such as CaO or β-$Ca_3(PO_4)_2$ supported the assumption of phase-pure HA [14] (see Suppl. 1.2, Fig. S2). EDS measurements revealed a Ca/P ratio of the coating of 1.67 (see Suppl. 1.3, Fig. S3), the theoretical value for stoichiometric HA. According to the criteria by Landi et al. [15], the crystallinity was calculated from the observed intensity $V_{112/300}$ of the hollow between the (112) and (300) reflections (at $2\Theta = 32.2°$ and $2\Theta = 32.9°$) and the intensity $I_{300}$ of the (300) peak. The application of the formula $X_C \approx 1 - (V_{112/300} / I_{300})$ resulted in a crystallinity $X_C$ of the as-precipitated and dried product of about 70% (Fig. 1a), while the sintered powder showed a crystallinity of more than 95% (see Suppl. 1.2, Fig. S2).

Fig. 1b shows the diffraction pattern of the sensor coating after EPD and immersion in SBF: crystalline structure and phase purity of the original powder were successfully maintained during deposition.

The surface roughness parameters $S_a$ of the PVD coatings were determined by AFM measurements (Fig. 2a–d) and were approximately the same for gold, Ti, and TiN (1.013 nm, 1.532 nm, and 0.989 nm, respectively), while the roughness of TiAgN was significantly higher ($S_a = 4.686$ nm). Composition and crystallographic properties of the PVD coatings were analyzed by XRD and compared to an uncoated chip with a plain gold surface (Fig. 2e). The diffraction pattern of the

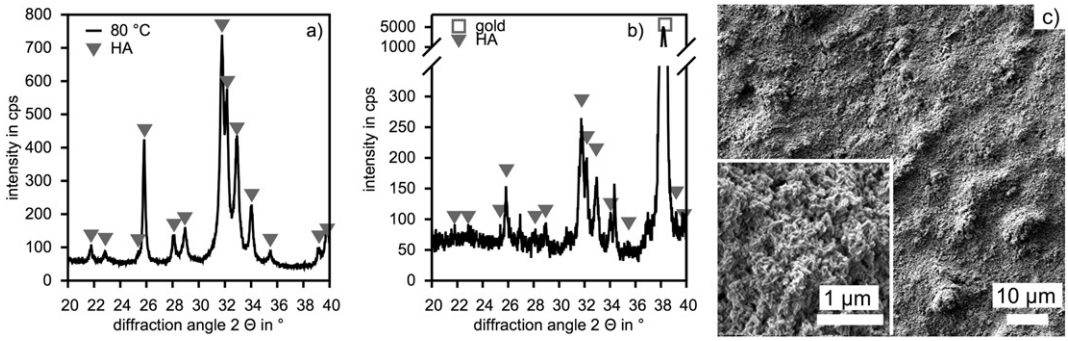


**Fig. 1.** Diffraction patterns of the as-precipitated powder (a) and the deposited and densified coating (b). SEM micrograph of the final coating (c).

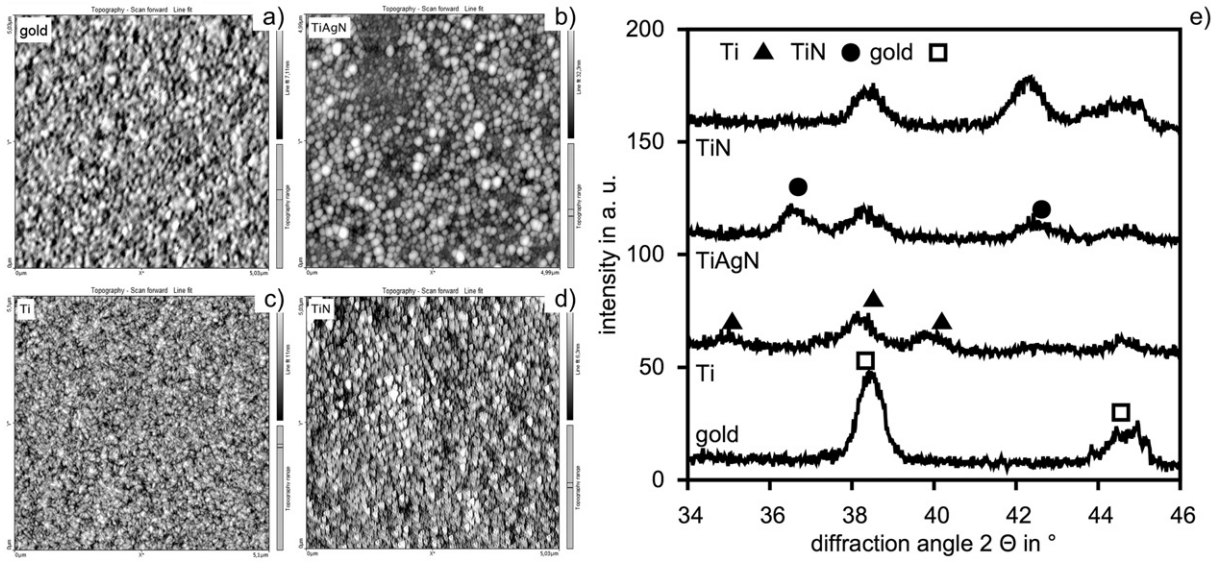


**Fig. 2.** (a)–(d): AFM images of the coatings deposited by PVD and the reference gold surface. (e) Diffraction patterns of PVD-coatings.

gold sensor surface showed two pronounced peaks at 2Θ = 38.2° and 44.4°, which could be clearly attributed to the (111) and the (200) lattice planes. The XRD pattern of the Ti coated sensor showed three distinct peaks around 35.1°, 38.2°, and 40° which could be attributed to the (100), (002), and (101) lattice planes of Ti, but apparently also the two gold peaks were present. Both, TiN and TiAgN patterns revealed the characteristic (200) peak of TiN, while the (111) peak did not appear in the pattern of the Ag-free coating, indicating a pronounced in-film

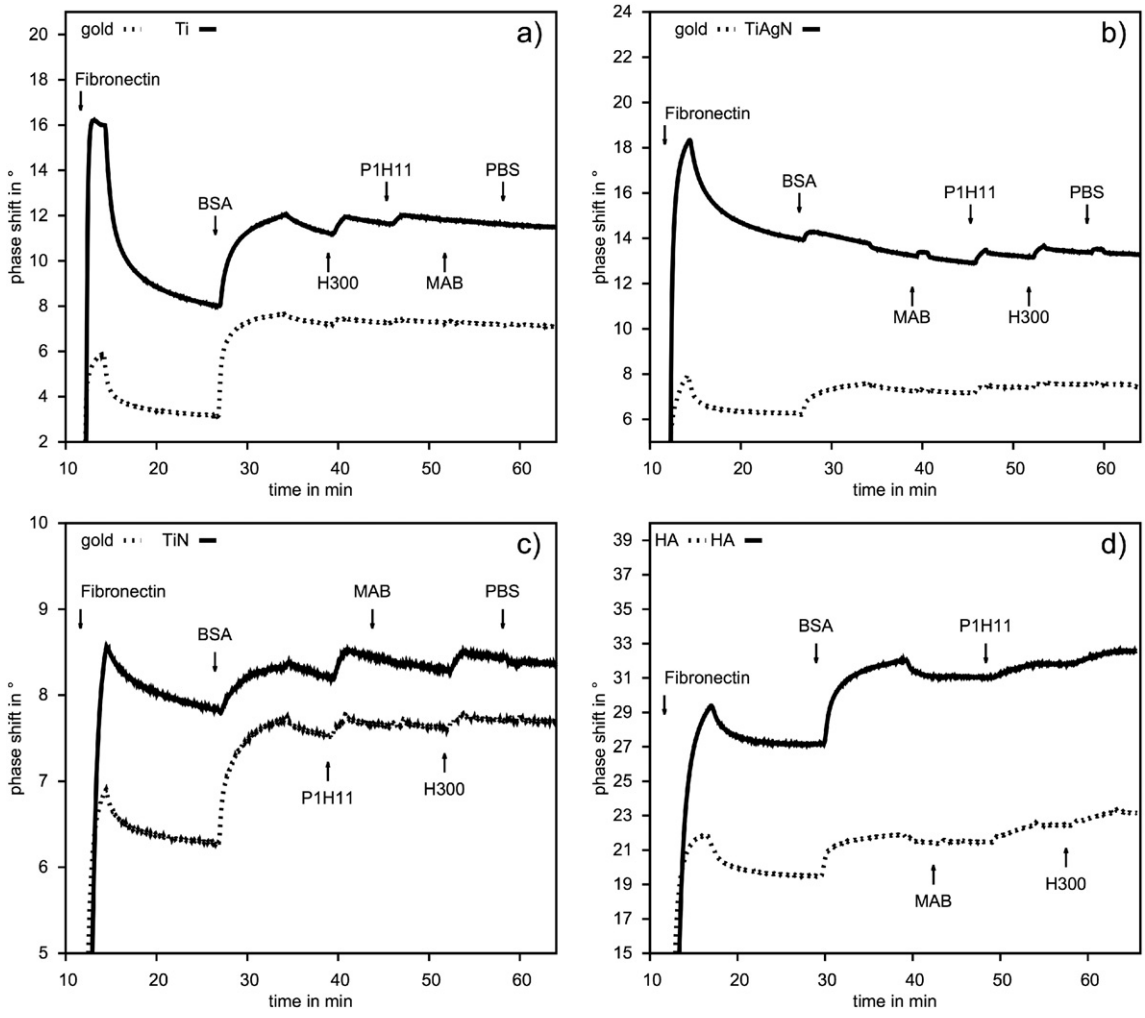


**Fig. 3.** Phase-shift vs. time for fibronectin adsorption to the coated chips and subsequent addition of the antibodies MAB, P1H11 and H300 in varying sequences.

texture. The results of additional X-ray photoelectron spectroscopy measurements supported the assumption that the silver was incorporated in its metallic state [16] (see Suppl. 1.4 and Fig. S4).

Fibronectin was used as a model protein for adsorption experiments. Fig. 3 shows the phase shifts of the SAW biosensor recorded over time for the different coating systems. After the injection of fibronectin and BSA the phase shift evolution followed a typical adsorption/desorption curve on all sensor surfaces. Furthermore, permanent binding of FN and BSA could be concluded from the phase shifts maintaining a certain level after the protein injections had stopped and the surface was rinsed with PBS. In all cases of antibody injections only H300 and P1H11 led to significant binding signals, whilst after the injection of MAB the phase shift stayed on the same level as for pure PBS. Fig. 3 shows examples of defined permutations of the series of antibody injection; nevertheless, additional experiments with changed injection sequences (data not shown) led to the same results. Apparently, the C-terminus, representing the binding site for H300 and the cell-binding domain, being the epitope for P1H11, were accessible for the antibodies, whilst the MAB antibody did not bind to the N-terminus of FN in any of the experiments. Hence, it can be concluded, that the binding of FN occurred via its N-terminus on all surfaces under investigation, thus blocking it for coupling of MAB. This was in good agreement with former measurements with QCM-D and ELISA-tests, which were carried out on PVD-sputtered titanium films [17]. Furthermore, Pohl et al. studied mineralization processes on commercially available carboxylate-SAM and on peptides derived from enzymes involved in biomineralization [18]. It would be most promising to transfer these experiments to the coatings presented in our study.

## 4. Conclusions

The SAW technique was successfully applied to metallic and CaP coatings produced by PVD and EPD on SAW biosensor chips. Chips were coated with Ti, TiN, TiAgN, and hydroxyapatite. An EPD setup was developed and a standard coating routine was established, suitable for the reproducible deposition of a variety of ceramic films. This novel technique enables the SAW device to be applied to manifold interesting systems, combining its high sensitivity to liquid-surface interactions with the possibility of time-resolved adsorption studies. Hence, the SAW technique can be regarded as a highly promising tool for studying complex interactions between metallic and ceramic surfaces and biochemical and biological species with high sensitivity. However, further studies are necessary, in order to thoroughly investigate the characteristics of wave propagation in deposited films and the influences of surface crystallography and topography on the resulting phase shift. This could make the surface acoustic wave technique a suitable method for exact quantitative adsorption analysis.

## Acknowledgements

We gratefully acknowledge financial support by DFG State Major Instrumentation Programme, funding the electron microscope Zeiss CB 340 (INST 105022/58-1 FUGG).

## Appendix A. Supplementary data

Supplementary data to this article can be found online at http://dx.doi.org/10.1016/j.msec.2015.12.075.

## References

[1] I.M. Rocha-Gaso, Y. Jiménez, L.A. Francis, A. Arnau, in: T. Rinken (Ed.), State Art Biosens. Gen. Asp. InTech, 2013.
[2] K. Länge, B.E. Rapp, M. Rapp, Anal. Bioanal. Chem. 391 (2008) 1509.
[3] N. Bracke, S. Barhdadi, E. Wynendaele, B. Gevaert, M. D'Hondt, B. De Spiegeleer, Sensors Actuators B Chem. 210 (2015) 103.
[4] M.D. Schlensog, T. Gronewold, M. Tewes, M. Famulok, E. Quandt, Sensors Actuators B Chem. 101 (3) (2004) 308.
[5] M. Pepeet, S. Glass, T. Gronewold, A. Kiwitz, A. Malavé, I. Stoyanov, M. Tewes, E. Quandt, Anal. Lett. 39 (8) (2006) 1747.
[6] J.W. Grate, S.J. Martin, R.M. White, Anal. Chem. 65 (1993) 940A.
[7] J. Andrä, A. Böhling, T.M.A. Gronewold, U. Schlecht, M. Perpeet, T. Gutsmann, Langmuir 24 (2008) 9148.
[8] R. Narayan (Ed.), Materials for Medical Devices, ASM International, 2012.
[9] A. Ewald, S.K. Glückermann, R. Thull, U. Gbureck, Biomed. Eng. OnLine 5 (2006) 22.
[10] C. Moseke, U. Gbureck, P. Elter, P. Drechsler, A. Zoll, R. Thull, A. Ewald, J. Mater. Sci. Mater. Med. 22 (2011) 2711.
[11] T. Schmitz, F. Warmuth, E. Werner, C. Hertl, J. Groll, U. Gbureck, C. Moseke, Mater. Sci. Eng. C 44 (2014) 126.
[12] A. Monkawa, T. Ikoma, S. Yunoki, T. Yoshioka, J. Tanaka, D. Chakarov, B. Kasemo, Biomaterials 27 (2006) 5748.
[13] T. Kokubo, H. Kushitani, S. Sakka, T. Kitsugi, T. Yamamuro, J. Biomed. Mater. Res. 24 (1990) 721.
[14] J.C. Elliott, Structure and Chemistry of the Apatites and Other Calcium Orthophosphates, Elsevier, 1994.
[15] E. Landi, A. Tampieri, G. Celotti, S. Sprio, J. Eur. Ceram. Soc. 20 (2000) 2377.
[16] H. Ju, J. Xu, Appl. Surf. Sci. 355 (2015) 878.
[17] C. Moseke, A. Ewald, Mater. Werkst. 40 (2009) 36.
[18] A. Pohl, I.M. Weisse, J. Beilstein, Nanotechnology 5 (2014) 1823.